Liquid Jet Impingement Cooling with Diamond Substrates for Extremely High Heat Flux Applications

John H. Lienhard V
Department of Mechanical Engineering
Massachusetts Institute of Technology
Cambridge, MA 02139 USA

Ali M. Khounsary
Advanced Photon Source
Argonne National Laboratory
Argonne, IL 60439

ABSTRACT

The combination of impinging jets and diamond substrates may provide an effective solution to a class of extremely high heat flux problems in which very localized heat loads must be removed. Some potential applications include the cooling of high-heat-load components in synchrotron x-ray, fusion, and semiconductor laser systems.

Impinging liquid jets are a very effective vehicle for removing high heat fluxes. The liquid supply arrangement is relatively simple, and low thermal resistances can be routinely achieved. A jet's cooling ability is a strong function of the size of the cooled area relative to the jet diameter. For relatively large area targets, the (area-averaged) critical heat fluxes can approach 20 W/mm^2. In this situation, burnout usually originates at the outer edge of the cooled region as increasing heat flux inhibits the liquid supply.

Limitations from liquid supply are minimized when heating is restricted to the jet stagnation zone. The high stagnation pressure and high velocity gradients appear to suppress critical flux phenomena, and fluxes of up to 400 W/mm^2 have been reached without evidence of burnout. Instead, the restrictions on heat flux are closely related to properties of the cooled target. Target properties become an issue owing to the large temperatures and large temperature gradients that accompany heat fluxes over 100 W/mm^2. These conditions necessitate a target with both high thermal conductivity to prevent excessive temperatures and good mechanical properties to prevent mechanical failures.

Recent developments in synthetic diamond technology present a possible solution to some of the solid-side constraints on heat flux. Polycrystalline diamond foils can now be produced by chemical vapor deposition in reasonable quantity and at reasonable cost. Synthetic single crystal diamonds as large as 1 cm^2 are also available. In addition to a thermal conductivity as high as five times that of copper, diamond possesses substantial mechanical strength and a low thermal expansion coefficient, all of which help to minimize thermal stress problems.

This paper considers the potential of jet/diamond systems for removing localized high heat fluxes. Diamond substrates are compared to other candidate materials. Limits on usable thermal resistances and heat transfer rates are estimated.

1. INTRODUCTION

Liquid jets are easily created by allowing a pressurized liquid to flow through a nozzle into a surrounding gas. The nozzle can be as simple as the end of a straight pipe or it can be a contracting design that accelerates the flow or damps turbulence. In either case, a high velocity column of liquid is formed, and this column can travel outward for many nozzle diameters before atomization breaks the jet into a spray. Prior to breakup, a jet provides a concentrated stream of liquid that is very effective for cooling surfaces.

A jet that impinges normally onto a hot surface supplies coolant directly to the region of the surface surrounding the stagnation point. As the liquid strikes the target, it turns ninety degrees and flows radially outward along the target surface (Figure 1). The downward impact of liquid followed by this outward removal produces an exceptionally thin boundary layer in the stagnation zone. As a result, the heat transfer coefficient, h, in jet impingement is very high, and impinging liquid jets are able to remove large heat fluxes with relatively low driving temperature differences.

When the jet velocity, u_f, is increased above 50 m/s, the liquid pressure in the stagnation zone can reach tens of atmospheres (rising as $\rho u_f^2/2$, for ρ the liquid density). At these pressures, the wall temperature required for vapor nucleation is significantly higher than at lower pressures. Hence, high-speed impinging jets can lead to a large wall-to-liquid temperature difference in addition to a high local heat transfer coefficient, resulting in extremely high heat flux removal from the stagnation zone. In this case, the cooling mechanism is some combination of convection and convective boiling. Fluxes in the range of 50–400 W/mm^2 have been reported[1], and higher values may be attainable.

A submerged liquid jet — one that issues into liquid rather than a into gas — will exhibit similar stagnation zone phenomena only if the nozzle is placed within a diameter or so of the target. If the nozzle is distant from the target, the jet's momentum is diffused into the surrounding liquid and cooling is generally less efficient. Our focus hereinafter is on unsubmerged jets.

1.1 High heat flux problems and jets

High heat flux situations that pose significant technical challenges can involve moderately high loads distributed over large areas or extremely high fluxes imposed over small areas. Problems like these arise in removing absorbed or internally-generated heat from high-power laser system components, synchrotron x-ray components, plasma diverters in nuclear fusion reactors, high-power laser diode arrays, linac radio-frequency microcavities, densely-packed electronic packages, hypersonic nozzle throats, and so on. Impinging jets are particularly useful in those situations where a very localized, high heat load must be removed.

A closely related problem in which efficient cooling is required is that of removing a moderately high heat load while maintaining a minimal temperature or temperature difference within the system. This situation occurs, for example, in semiconductor laser systems, where junction temperatures must be held below about 150°C while heat flux may exceed 10 W/mm^2. Such cooling is also necessary for highly heated grazing-incidence x-ray mirrors in order to maintain the thermal deformation within a high precision tolerance. In these designs, a very high heat transfer coefficient must be achieved,

even though the heat flux itself may not be very high. The large h of jet impingement is potentially useful in these cases as well.

It should be emphasized that high heat transfer coefficients can be achieved and measured without having a high heat flux. Routine impinging jet experiments, for example, may produce heat transfer coefficients of $h = 0.1$ W/mm^{2}K or more; however, if the temperature difference is limited (to about 5°C, say), the heat flux remains moderate, e.g. $q = h\Delta T \approx 0.5$ W/mm^2.

1.2 Factors that limit heat flux removal

The maximum heat flux that can be removed from a system depends on several factors: the maximum heat transfer coefficient achievable in the coolant stream; the minimum achievable conduction resistance in the target being cooled; and the maximum temperature allowed in the material comprising the system.

1.2.1 Limits imposed by h

The heat transfer coefficient is normally limited by the critical heat flux, or CHF, at which nucleate boiling gives way to film boiling, because CHF often decreases h markedly. The resultant increases in wall temperature may lead to burnout and destruction the cooled surface. The occurrence and impact of CHF depend strongly on how well liquid can be supplied to the heated surface, and thus they can depend on the size of the area being cooled. In some convective boiling situations involving small heated areas (of a few square millimeters), CHF has been observed to cause only a modest decrease in h and burnout does not accompany it; however, this is less often true for larger areas.

For impingement cooling, both the area-average CHF and the area-average heat transfer coefficient have been found to depend strongly on the diameter of the heated section of the target relative to the diameter of the coolant jet. For water jets cooling large targets (having heated diameters of 5 to 10 times jet diameter), burnout occurs at critical heat fluxes of only 5–20 W/mm^2. When heating is confined to the stagnation zone (a heated diameter of less than about 1.5 times the jet diameter), CHF is has not been observed to be a limitation, even for heat fluxes as high as 400 W/mm^2.

1.2.2 Limits imposed by the conduction resistance

The liquid-side thermal resistance, $1/h$, is in series with a solid-side conduction resistance. The conduction resistance depends on the thermal conductivity of the target material, k, and on the target geometry. The latter may be characterized one-dimensionally as target thickness, t, so that the conduction resistance is t/k. Thermally, we should like to minimize the thickness; however, structural requirements on the target usually limit our ability to do so. Maximum thermal conductivity is clearly desirable as well, but it is determined by the choice of target material.

1.2.3 Limits imposed by the maximum temperature and target material

In addition to the limits on convective and conductive resistance, a particular system will have an upper temperature that should not be exceeded. This may be a relatively low temperature (as for the semiconductor junction case mentioned above) or it may be a relatively high temperature beyond which the target material softens, melts, fractures, or decomposes. This temperature limit, together with the thermal resistance limits, sets the maximum heat flux that a system can carry.

The maximum temperature and the thermal conductivity of the target must be examined jointly with the thermal stresses or deformation that occur. For example, in jet impingement experiments at extremely high heat fluxes, thermal stresses (causing fracture and buckling) and high-temperature yielding have often been the cause of target failure, owing to the high temperatures and high temperature gradients occurring. An increase in heat flux in this situation hinges on obtaining materials with either greater thermomechanical strength or higher thermal conductivity (the latter serving to lower temperature gradients). In this sense, synthetic diamond foils are among the most promising substances, as described in later sections of this paper.

In another situation, if a moderate flux is to be removed with a low maximum system temperature, minimization of the thermal resistances will instead be critical. Here again, the jet-diamond combination is a very promising design as a result of the high h of jet impingement and the low k of diamond.

2. HEAT TRANSFER IN JET IMPINGEMENT

2.1 Convective heat transfer

The convective heat transfer coefficient, h, in nonboiling jet impingement has been measured in several recent studies. The results and accompanying theory show h to be a maximum within the stagnation zone and to decrease rapidly with radius outside the stagnation zone. The radius of the stagnation zone is found to be $r \approx 0.7d$, where d is the diameter of the jet prior to impact.

The actual value of h in the stagnation zone depends primarily on the jet Reynolds number, $\mathrm{Re}_d = u_f d/\nu$, and the liquid Prandtl number, $\mathrm{Pr} = \nu/\alpha$, for ν the liquid kinematic viscosity and α the liquid thermal diffusivity. The velocity profile across the jet and the distance of the nozzle from the target can also affect h.

For jets issuing from long tubes, the flow will be turbulent for Re_d above 2000–4000. A typical result for stagnation zone heat transfer is[2]

$$\mathrm{Nu}_d \equiv \frac{hd}{k} = 0.278\,\mathrm{Re}_d^{0.633}\,\mathrm{Pr}^{1/3}, \tag{1}$$

which is valid for fully turbulent jets of nonmetallic liquids ($\mathrm{Pr} > 1$) and Re_d between 25,000 and 85,000. Such results show that the heat transfer coefficient is larger for smaller diameter jets and increases with jet velocity, owing to thinning of the boundary layer.

For laminar jets, the jet can be smaller than the nozzle diameter if the nozzle produces a strong contraction (as does a sharp-edged orifice). A laminar jet's velocity profile is also very sensitive to the nozzle shape. For jets issuing from tubes at $\mathrm{Re}_d < 2000 - 4000$, the profile is parabolic, while for jets issuing from sharp-edged orifices at any Re_d, the profile is uniform after the jet contracts. Nonuniform velocity profiles can more than double the stagnation zone heat transfer, provided that the nozzle is placed within a few nozzle diameters of the target, so that the profile is unable to dissipate toward the mean jet velocity. For example, a parabolic-profile laminar jet has

$$\mathrm{Nu}_d = 1.648\,\mathrm{Re}_d^{1/2}\mathrm{Pr}^{0.368}, \tag{2}$$

$(1 \leq \mathrm{Pr} \leq 10)$ while a uniform profile laminar jet has

$$\mathrm{Nu}_d = 0.745\,\mathrm{Re}_d^{1/2}\mathrm{Pr}^{1/3} \tag{3}$$

$(\mathrm{Pr} \geq 1)$.[3] For turbulent jets, the jet diameter and the nozzle diameter are essentially equal for many nozzle types and the velocity profile is more nearly uniform.

For jets of metallic liquids ($\mathrm{Pr} < 0.15$), a theoretical result is available[3]:

$$\mathrm{Nu}_d = \frac{hd}{k} = \frac{1.079}{1 + 0.6419\sqrt{\mathrm{Pr}}}\mathrm{Re}_d^{1/2}\mathrm{Pr}^{1/2}. \tag{4}$$

This equation should approximate cases of relatively uniform velocity profiles in either laminar or turbulent flow. Various other results for the h of laminar jets are summarized by Liu et al.[3]. Results for h downstream of the stagnation zone are given by Liu et al.[4] for laminar jets and by Lienhard et al.[5] for turbulent jets. It should also be noted that modest levels of wall roughness may increase the impingement heat transfer coefficient 50% or more.[2]

2.2 Boiling in jet impingement

Nucleate boiling raises the impingement heat transfer coefficient markedly, at least in certain configurations.[6] The liquid may boil when the wall temperature exceeds the saturation temperature at the local pressure. The elevated liquid pressure at the stagnation point tends to suppress phase change there, but pressure returns to ambient pressure by a radius of about one jet diameter from the stagnation point. Thus, boiling typically begins at the outermost radius of the cocled surface where the liquid pressures are low and the wall temperatures are generally highest. Critical heat flux and burnout usually occur when boiling dries up the outflowing liquid sheet at the outer radius of the cooled target.

If heating is instead confined to the stagnation region, high pressure is maintained over the entire hot portion of the target and the wall temperature required for nucleation is greater. At present, less is known about boiling and CHF processes in this configuration, even though it may be ideal for hot-spot cooling. Estimated heat transfer coefficients for this configuration[1] have exceeded 1 $\mathrm{W/mm^2K}$.

3. CRITICAL HEAT FLUX AND JETS

CHF in forced convection boiling depends on the configuration of the flow and the heated region. The highest CHF values obtained have generally been those occuring in tube flows of water, with maximum critical fluxes in the range of 100 to 350 W/mm^2. Usually, these critical fluxes are reached under large subcooling of the bulk liquid[7] by making the tube diameter small (a millimeter or two) and increasing the flow velocity to as much as 50 m/s. Even at these extreme conditions, the region over which high heat flux occurs is limited to a few centimeters along the length of the tube.

For liquid jet impingement, most studies of critical heat flux to date have focused on relatively large ratios of heated-region diameter to jet diameter. Very little data is available in regard to boiling situations in which heating is confined to the stagnation region. As noted, the two situations are not likely to be similar because large heater surfaces generally exhibit dryout at large radii, whereas heater surfaces smaller than the stagnation zone experience better liquid supply and higher pressures.

3.1 Jet CHF for large area targets

Most of the available CHF data for jet impingement has been obtained by Katto, Monde, and coworkers[8–10] using jets of freon or water impinging on targets of 5 to 60 jet diameters in diameter. Nucleation was observed over a large radial band of the heater covering most of its surface downstream of the stagnation zone. Nucleation was not reported in the stagnation zone itself, although it was described as being within a diameter of it. CHF generally began at the outer edge of the heated disk and was often accompanied by dryout. Area-average critical heat fluxes of up to 18 W/mm^2 were reported.

Several models and correlations have been developed for CHF in the jet/disk configuration.[11,12] These models show that vapor efflux and droplet ejection are critical to the burnout process. The ejection of droplets (by vapor bubbles) increases substantially with increasing heat flux and limits the supply of liquid to larger radii. It should be noted, however, that droplet splattering is now also known to occur as a kinematic phenomenon in isothermal jet impingement.[5,13] This effect will probably reduce the CHF on large area targets when the jet velocity is increased into the range of kinematic splatter.

Arrays of jets have been implemented as a method of cooling still larger areas. This configuration has been studied by Monde and Inoue[14], who found that array CHF behavior was actually quite similar to single jet CHF. In particular, the single jet correlations of Monde[10] and of Sharan and Lienhard[11] accurately predict the area-average CHF of jet arrays having as many as four jets.

3.2 Jet CHF for stagnation zone heating

When heating is restricted to the stagnation zone, the dryout phenomena that occur in large target cooling are no longer an issue. Nucleation behavior in this case, however, remains sketchy, and two questions appear to be central to the understanding of stagnation zone CHF: how the very high local liquid pressure will affect the critical heat flux, and how boiling and CHF phenomena occur when heating is limited to a small area.

At high velocities, the stagnation point pressure can become a significant fraction of the liquid's critical pressure, p_c. Thermodynamic effects should be significant, in the sense of strongly altered physical properties and nucleation dynamics. Past work in various other boiling configurations has established that increasing pressure raises both the nucleate boiling heat flux (at a given wall superheat) and the critical heat flux.[15,16] Maximum CHF occurs for pressures in the vicinity of $0.35p_c$, with rapidly decreasing CHF for pressures beyond $0.4p_c$. For water, this maximum CHF corresponds to pressures of about 70 atm in both pool and convective boiling.[17] For an impinging water jet, a stagnation point pressure of 70 atm occurs at a jet speed of about 120 m/s. It seems reasonable to expect that heat flux (boiling and critical heat flux, as well as convective flux) will increase as jet speed is increased toward this value. Indeed, Liu and Lienhard[1] observed a monotonic increase in stagnation point heat flux (at fixed wall superheat) as jet velocities were increased from 50 to 134 m/s.

A few studies have also examined boiling behavior for small heater sizes. Ma and Bergles[6] provide measurements of nucleate boiling heat fluxes during jet impingement of R-113 on a square heated region with a dimension of 2 to 3 jet diameters. While they reported a trend toward a velocity-independent fully developed boiling curve as the flux increased, the velocities involved (10 m/s or less) were too low to cause a thermodynamically significant increase in the stagnation point pressure. They did not provide direct data for CHF. Samant and Simon[18] examined boiling behavior from a small heated patch cooled by a parallel turbulent channel flow of FC-72. They saw no evidence of a burnout phenomenon at CHF; instead, the heat flux simply increased more slowly with increasing wall superheat in the transition and film boiling regions than in the nucleate regime.

4. EXTREMELY HIGH HEAT FLUXES IN JET IMPINGEMENT

Liu and Lienhard[1] made a direct attempt to create extremely high heat fluxes using high velocity water jets to cool a small heated region. They confined the heating to the high pressure stagnation region of a 1.9 mm diameter jet, so as to capitalize on the thermodynamic suppression phase change. Jet velocities ranged from 50 to 134 m/s, and associated stagnation pressures were between 12 and 89 atm. Their heat fluxes ranged between 50 and 400 W/mm^2.

Those experiments used thin metal targets heated by a plasma arc on one side and cooled by the jet on the opposite side. The arc-side of the target was partially melted; temperatures through the target varied from the melting point temperature to a value of 100–300°C on the liquid side. In this condition, the targets were less than a millimeter in thickness.

Upon impact, the jets splattered much liquid, which prevented direct visualization of the stagnation zone. Thus, it was not possible to verify the presence or absence of phase change. However, Liu and Lienhard saw no evidence of a CHF or burnout phenomenon during stagnation point heating. Their heat fluxes were generally limited by either the thermal power available for heating or by a mechanical failure of the targets (rupture in the form of fracture or plastic yielding). Failure depended on the target material used but not necessarily on its conductivity. The highest fluxes were achieved using molybdenum targets; targets of steel, tungsten, and tantalum all failed at lower heat fluxes. The absence of a burnout process and the material dependence of target failure imply that liquid-side processes are not the principal factor limiting heat removal in these conditions.

From an engineering viewpoint, the limitations on stagnation zone heat flux by jet impingement are associated with the structural integrity of the solid target rather than the heat transfer coefficient. Temperatures and temperature gradients in the targets are very high; thermal stresses are large; and the extremely high flux experiments to date show that mechanical failure of the target tends to limit the achievable heat flux. To obtain still higher fluxes, better target materials are needed.

5. MATERIAL LIMITATIONS ON HEAT FLUX

The target material is important in two contexts: experimental studies of CHF and practical application problems.

Experimentally, the need for targets that can withstand higher incident heat flux than has hitherto been possible is the key to exploring the upper limits on the CHF phenomena. The issue is the survivability of the target. The target must exhibit small conduction resistance (i.e., high thermal conductivity and small thickness) and high thermomechanical strength (high melting point, low thermal expansion coefficient, high stiffness at elevated temperatures, and so on).

As the thermal load on a target is increased, one of a few scenarios may arise. The thermal gradient across the thickness of the target (which, to a first approximation, is independent of the heat transfer coefficient) may reach such levels that the target fails under the resulting thermal stresses. Other possible failures include the loss of mechanical strength at elevated temperatures and partial melting of the target. These limitations preclude further exploration of higher CHF values.

From an applications point of view, the target material may be restricted to one or more substances that have the appropriate thermal, mechanical, and physical characteristics for particular components. Additionally, cooled components may impose restrictions on the flow velocity and pressure owing to vibration, pressure-induced distortions, system reliability, or other design and operation considerations.

From a purely experimental standpoint, a few materials stand out as promising candidates for targets in the investigation of higher CHF limits. Pyrolytic graphite and diamond are particularly interesting (see Table 1). Ordinary graphite can survive very high temperatures but has a low thermal conductivity. Pyrolytic graphite, on the other hand, can have very high directional thermal conductivities (to over three times that of copper) but with correspondingly reduced mechanical strength. The promise of pyrolytic graphite for the present experiments lies, perhaps, in its anisotropy. This allows for efficient transfer of heat through the thickness of the target with little lateral heat transfer. Because fin conduction effects are minimized, the heat transfer is effectively limited to the area right below the heated region, making it possible to confine the heating to the high-pressure, jet stagnation region.

Diamond, in contrast to graphite, has a uniform thermal conductivity, low thermal expansion coefficient, and high strength[19–22], all of which make it a suitable candidate for studies of extremely high heat flux jet impingement.

In a practical context, advances in synthetic diamond technology have opened the door to a host of interesting engineering applications. The high thermal conductivity of diamond and, often, its

low thermal expansion coefficient and high strength make it an attractive material for many thermal management problems in which effective dissipation and removal of heat from "hot spots" is sought. Small size, industrial, single crystal diamonds, have long been used as the heat-sink material in high-power laser diode applications.[23] Large-area polycrystalline diamonds recently produced by the chemical vapor deposition (CVD) processes are finding more widespread use in many thermal management problems. Another area that can significantly benefit from the emerging diamond technology is synchrotron radiation engineering, in which thermal management of various components subjected to the extremely high heat flux of the x-ray beams is quite challenging.[24–28]

5.1 Material figures of merit

Additional support for the use of diamond in extremely high flux experiments can be found in figures of merit for thermal stress and heat condcution. Thermal stress depends in a detailed way on the mechanical configuration of the target and on temperature distribution within it; however, for a thin plate having a temperature drop ΔT through its thickness, the maximum thermal stress is on the order of $E\alpha\,\Delta T/(1-\nu)$, where symbols are defined in Table 1. Two possible figures of merit compare this stress to yield strength, σ_Y, and tensile strength, σ_T. Since ΔT is inversely proportional to conductivity (for a given flux), a stress figure of merit is, for example

$$\mathrm{SFM} = \frac{\sigma_Y k(1-\nu)}{E\alpha} \tag{5}$$

For metals, the stress figure of merit will vary substantially with alloying, processing, and operating temperature.

A second figure of merit addresses conduction through the target, which is limited by the material conductivity and the maximum allowable material temperature. With a nominal minimum temperature of 0°C, this figure of merit is

$$\mathrm{CFM} = k(T_{max} - 0°\mathrm{C}) \tag{6}$$

For metals, melting point temperature and mean-temperature thermal conductivity can be used; for synthetic diamond, a decomposition temperature of 700°C is used.

The figures of merit are tabulated in Table 2 for several candidate materials. Diamond has by far the highest value in both categories.

6. EXPLORING EXTREMELY HIGH FLUX COOLING WITH DIAMOND

In the exploration of extremely high heat flux cooling by jet impingement, and in further examination of jet CHF phenomena, the experimental arrangement shown in Figure 2 may be used. A CO_2 laser of several kilowatts will be used as the heat source. It is directed at the rear of a thin diamond target that is cooled from the opposite side by a water jet.

The laser beam will be focused to a diameter of 1 mm. The target may be coated with an infrared absorbent film, such as tungsten, so that heating occurs at the surface of the target. Alternatively, a

Table 1: Single crystal diamond properties and typical solid pyrolytic graphite properties at room temperature.[19–22] For graphite, the C axis is normal to the graphite planes, and the A and B axes are parallel to the graphite planes.

Property	Diamond	Graphite
Atomic number	6	6
Density (g/cm^3)	3.5	2.2
Thermal conductivity, k (W/cm-K)	≈ 21	A/B 3.5
		C 0.02
Thermal expansion coefficient, α ($K^{-1} \times 10^{-6}$)	0.8	A/B 1.7
		C 22
Specific heat (J/kg-K)	520	1600
Thermal diffusivity (cm^2/s)	≈ 11.5	A/B 1.0
		C 0.006
Young's modulus, E (GPa)	1,050	A/B 28
		C 11
Poisson's ratio, ν	0.1-0.29	ν_{AB} −0.15
		ν_{AC} 0.90
		ν_{CA} 0.35
Melting point (°C)	4300	3600
Tensile strength, σ_T (MPa)	> 3000	A/B 100
		C 2
Yield strength, σ_Y (MPa)	NA	100

Table 2: Representative stress figure of merit (SFM) and conduction figure of merit (CFM) for several materials. SFM at room temperature unless otherwise indicated.

Material	SFM, yield (kW/m)	SFM, tensile (kW/m)	CFM (kW/m)
Diamond	—	6000	1470
Copper (annealed)	3.3	21	418
Molybdenum (annealed)	21	22	235
	9.5 (400°C)	13 (900°C)	
Molybdenum (wrought)	31	46–78	
Tungsten (annealed)	14	31	375
	2.4 (1500°C)	4.8 (1500°C)	
Tungsten (Ni/Fe alloy)	28	39	
Steel (low carbon)	3	4	45

slightly different approach may be taken allowing laser power to be absorbed within the target itself. The diamond target thickness will be about 1 mm. The jet will have a nozzle diameter of about 2 mm and speeds in the range of 50 to 200 m/s.

Calorimetry may be accomplished using pyrometric measurements. On the laser side, the pyrometric wavelengths should be separated from the laser wavelength. Detection of the emission from the coating, together with knowledge of the coating emissivity could provide the target temperature. The liquid jet temperatures will be measured upstream of the nozzle using a resistance thermometer or thermocouple. The liquid-side surface temperature of the target can be bounded by various considerations related to phase change temperatures[1]; however, a direct measurement is preferable.

To accomplish this direct measurement, we may again turn to pyrometry. The problem is severely complicated by (i) the surface roughness and splattering of normal turbulent liquid jets, which will obstruct the view of the wall, and (ii) the absorption of infrared radiation by water. The splattering can be at least partially suppressed through the use of polymer additives that inhibit surface roughening and breakup of liquid jets. An alternative temperature measurement scheme might use a thin metal film deposited on the target in the stagnation zone that acts as a resistance thermometer.

6.1 Estimates of expected heat transfer

The range of conditions achievable in these experiments can be roughly estimated using the established characteristics of liquid jets and the known properties of diamond.

For a plate of thickness t and thermal conductivity k heated on one side ($x = 0$) by a uniform heat flux q'' and cooled on the opposite side ($x = t$) by a liquid at T_∞ with a heat transfer coefficient h, we have the following one-dimensional temperature distribution:

$$T(x) - T_\infty = q'' \left\{ \frac{(t-x)}{k} + \frac{1}{h} \right\}. \tag{7}$$

The heated side temperature is then

$$T(0) = T_\infty + q'' \left\{ \frac{t}{k} + \frac{1}{h} \right\}, \tag{8}$$

while the liquid-side temperature is

$$T(t) = T_\infty + \frac{q''}{h}, \tag{9}$$

and the temperature drop through the plate is

$$T(0) - T(t) = q'' \frac{t}{k}. \tag{10}$$

For a diamond layer of thickness 1 mm and an assumed thermal conductivity $k = 2.1$ W/mm-K, the hot-side temperature is

$$T(0) = T_\infty + q'' \left\{ \frac{1}{2.1} + \frac{1}{h} \right\}, \tag{11}$$

and the temperature drop is

$$T(0) - T(t) = q'' \frac{1}{2.1} \tag{12}$$

for q'' in W/mm^2.

Measurements of the heat transfer coefficient in the proposed range of Reynolds numbers (from 2×10^5 to 2×10^6) are fairly uncertain owing to the uncertainty in past data for the liquid-side wall temperature. The values suggested, however, are on the order of 0.5 to 1.3 W/mm^{2}K. We may alternatively make a rough estimate of the heat transfer coefficient by extrapolating Equation 1 and using an appropriate average boundary layer temperature. That calculation yields convective h values between 0.20 and 1.0 W/mm^{2}K.

The maximum operating temperature of synthetic diamond is roughly 700°C; beyond this temperature, synthetic diamond oxidizes and then graphitizes. Using this maximum temperature, taking a representative value of $h = 1.1$ W/mm^{2}K, and assuming the water is subcooled to $T_\infty \approx 0$°C, Equation (11) gives a maximum heat flux of 500 W/mm^2. The temperature drop through the diamond target will be 240°C (neglecting radial conduction). Thermal stresses will depend on the mechanical support used for the diamond, but bounding estimates suggest that the stresses will be well below the target's failure limits.

These estimates show that the diamond system can reach extremely high fluxes without encountering an obvious cause of wall failure, underlining its potential value in establishing the nature of liquid-side limitations to impingement cooling.

If phase change conditions evolve in the liquid and increase h further (toward a CHF of some type), Equation (11) shows that the diamond temperature will be significantly lowered. Thus, increasing h up to and over 2 W/mm^{2}K will have a significant impact on the diamond system.

In contrast, for a copper target ($t/k = 1/0.4$ mm^{2}K/W), raising h beyond 0.40 W/mm^{2}K will show only a diminishing return because the temperature (and stress) fields are dominated by the conduction resistance of the target. In other words, increasing h over 0.40 W/mm^{2}K will contribute little improvement to any metallic high heat flux system of similar dimensions.

These estimates suggest that diamond targets may prove to be indispensible for practical applications that can actually exploit the high h of jet impingement as a means of temperature control.

7. SUMMARY

This paper has examined the use of impinging liquid jets and synthetic diamond films in high heat flux applications. Both extremely high fluxes and extremely high heat transfer coefficients are possible in jet impingement, but the target material properties have posed a strong limitation on the fluxes achievable and have limited the identification of CHF phenomena. Diamond foils appear to provide a means of overcoming these two difficulties. The combination of impinging jets and diamond foils will be useful in both moderate heat flux situations requiring minimal thermal resistance and in extremely high heat flux situations for which temperature differences may be large. Estimates for the jet/diamond configuration have been made and an experimental configuration that tests these ideas has been proposed.

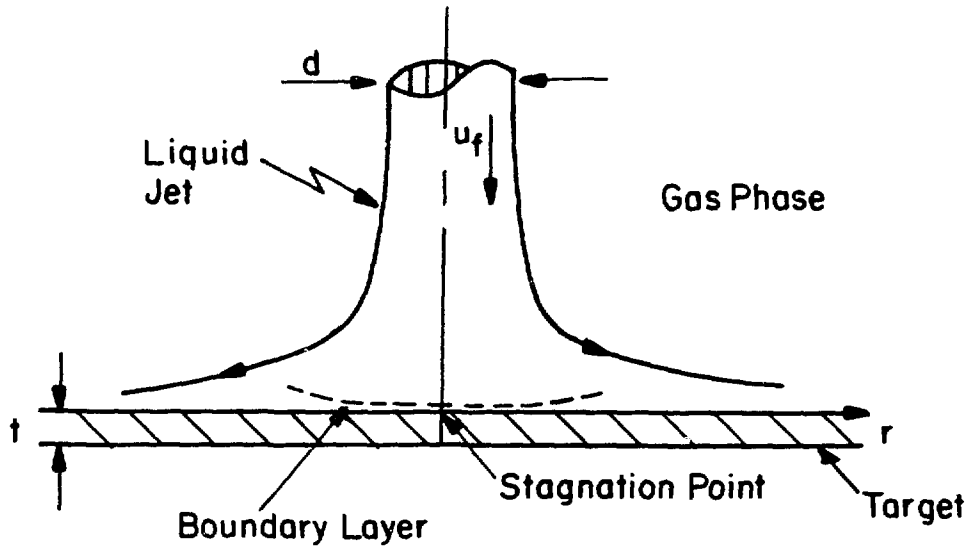

Figure 1: An Impinging Liquid Jet

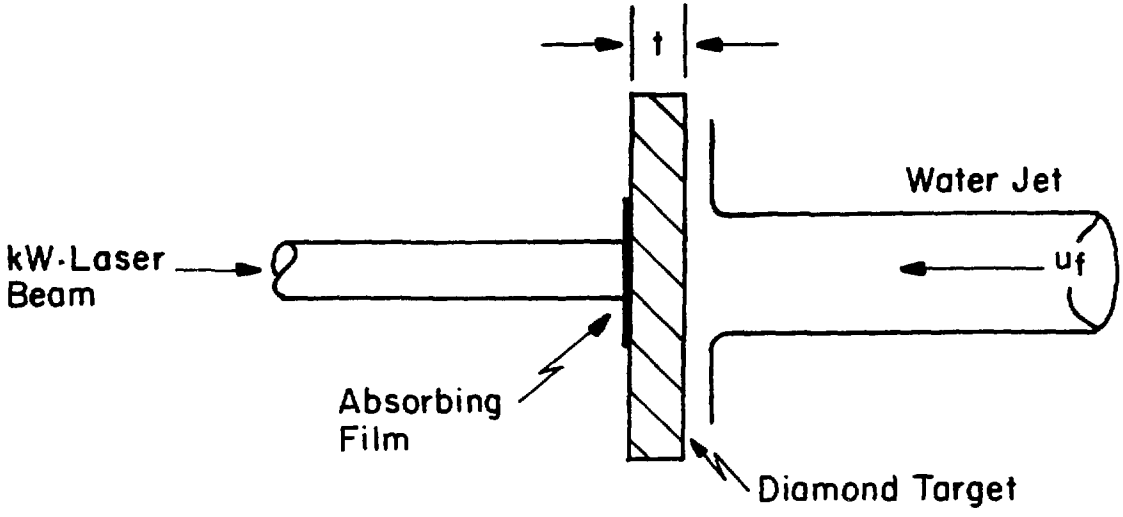

Figure 2: Proposed Experimental Arrangement

8. REFERENCES

1. X. Liu and J.H. Lienhard V, "Extremely High Heat Fluxes Beneath Impinging Liquid Jets," *J. Heat Transfer*, Vol. 115, pp.472–476, 1993.

2. L.A. Gabour and J.H. Lienhard V, "Wall Roughness Effects on Stagnation-Point Heat Transfer Beneath Impinging Liquid Jets," 29th ASME/AIChE National Heat Transfer Conference, Atlanta, August 1993.

3. X. Liu, L.A. Gabour, and J.H. Lienhard V, "Stagnation Point Heat Transfer During Impingement of Laminar Liquid Jets: Analysis with Surface Tension," *J. Heat Transfer*, Vol. 115, No. 1, pp.99–105, 1993.

4. X. Liu, J.H. Lienhard V, and J.S. Lombara, "Convective Heat Transfer by Impingement of Circular Liquid Jets," *J. Heat Transfer*, Vol. 113, No. 3, pp.571-582, 1991.

5. J.H. Lienhard V, X. Liu, and L.A. Gabour, "Splattering and Heat Transfer During Impingement of a Turbulent Liquid Jet," *J. Heat Transfer*, Vol.114, No.2, pp.362–372, May 1992.

6. C.-F. Ma and A.E. Bergles, "Jet Impingement Nucleate Boiling," *Intl. J. Heat Mass Transfer*, Vol.29, No.8, pp.1095–1101, 1986.

7. R.D. Boyd, "Subcooled Flow Boiling Critical Heat Flux (CHF) and Its Application to Fusion Energy Components. Part II: A Review of Microconvective, Experimental and Correlational Aspects," *Fusion Technology*, Vol.7, pp.31–52, Jan. 1985.

8. Y. Katto and M. Shimizu, "Upper Limit of CHF in the Saturated Forced Convection Boiling on a Heated Disk with a Small Impinging Jet," *J. Heat Transfer*, Vol.101, pp.265–269, May 1979.

9. M. Monde and Y. Katto, "Burnout in a High Heat-Flux Boiling System With an Impinging Jet," *Intl. J. Heat Mass Transfer*, Vol.21, pp.295–305, 1978.

10. M. Monde, "Critical Heat Flux in Saturated Forced Convection Boiling on a Heated Disk with an Impinging Jet," *J. Heat Transfer*, Vol.109, pp.991–996, November 1987.

11. A. Sharan and J.H. Lienhard, "On Predicting Burnout in the Jet-Disk Configuration," *J. Heat Transfer*, Vol.107, pp.396–401, May 1985.

12. M. Kandula, "Mechanisms and predictions of burnout in flow boiling over heated surfaces with an impinging jet," *Intl. J. Heat Mass Transfer*, Vol.33, No.9, pp.1795–1803, 1990.

13. S.K. Bhunia and J.H. Lienhard V, "Splattering during Turbulent Liquid Jet Impingement on Solid Targets," *J. Fluids Engineering*, Vol. 116, (in press), 1994.

14. M. Monde and T. Inoue, "Critical Heat Flux in Saturated Forced Convective Boiling on a Heated Disk with Multiple Impinging Jets," *J. Heat Transfer*, Vol.113, pp.722–727, August 1991.

15. J.H. Lienhard and V.E. Schrock, "The Effect of Pressure, Geometry, and the Equation of State Upon the Peak and Minimum Boiling Heat Flux," *J. Heat Transfer,* Vol.85, No.3, pp.261–268, 1963.

16. K. Bier, H.R. Engelhorn, and D. Gorenflo, "Heat Transfer at Burnout and Leidenfrost Points for Pressures up to Critical," in E. Hahne and U. Grigull (editors), *Heat Transfer in Boiling.* Washington: Hemisphere Publishing Inc., 1977.

17. P.B. Whalley, Boiling, Condensation, and Gas-Liquid Flow. New York: Oxford University Press, 1987.

18. K.R. Samant and T.W. Simon, "Heat Transfer form a Small Heated Region to R-113 and FC-72," *J. Heat Transfer,* Vol.111, pp.1053–1059, November 1989.

19. R. Berman, Physical Properties of Diamond. Oxford: Clarendon Press, 1965.

20. J. Wilks and E. Wilks, Properties and Applications of Diamond. Butterworth Heinemann, 1991.

21. J.E. Field (ed.), The Properties of Diamond. New York: Academic Press, 1979.

22. J.T. Glass, R. Messier, and N. Fujimori (ed.s), Diamond, Silicon, Carbide, and Related Wide Bandgap Semiconductors, 1990.

23. M. Bernstein, "CVD Diamond: Taking the Heat," *Laser & Optronics*, April 1991.

24. Khounsary, A. M., J. J. Chrzas, D. M. Mills, and P. J. Viccaro, "Performance Analysis of High Power Synchrotron X-ray Monochromators," *Optical Engineering*, Vol. 29, pg. 1273, 1990.

25. A.M. Khounsary, "Applications of synthetic diamond in high-heat load synchrotron x-ray beamlines," *3rd Annual Diamond Technology Workshop*, Wayne State University, March 17-18, 1992.

26. A.M. Khounsary, R.K. Smither, and S. Davey, "Diamond Monochromator for High Heat Flux Synchrotron X-ray Beams," *SPIE Proceedings*, Vol. 1739, pp. 628-642, 1992.

27. A.M. Khounsary and W. Phillips, "Thermal, structural, and fabrication aspects of diamond windows for high power synchrotron x-ray beamlines," *Proc. of the SPIE's 1992 International Symposium on Optical Applied Science and Engineering*, Vol. 1379, 1992.

28. S. Sharma, L.E. Berman, J.B. Hastings, and M. Hart, "Adaptive optics for high power beamlines using diamond crystal monochromators," *SPIE Proceedings*, Vol.1739, pp. 604-614, 1992.